

See discussions, stats, and author profiles for this publication at: <https://www.researchgate.net/publication/231244641>

# Time-Resolved in Situ X-ray Powder Diffraction Study of the Formation of Mesoporous Silicates

ARTICLE in CHEMISTRY OF MATERIALS · JUNE 1999

Impact Factor: 8.35 · DOI: 10.1021/cm990044a

---

CITATIONS

50

---

READS

12

6 AUTHORS, INCLUDING:



**Stephen O'Brien**

City College of New York

**126** PUBLICATIONS **7,787** CITATIONS

SEE PROFILE



**Andrew M. Fogg**

University of Chester

**66** PUBLICATIONS **1,758** CITATIONS

SEE PROFILE



**Dermot O'Hare**

University of Oxford

**392** PUBLICATIONS **10,308** CITATIONS

SEE PROFILE

# Time-Resolved in Situ X-ray Powder Diffraction Study of the Formation of Mesoporous Silicates

Stephen O'Brien,<sup>†</sup> Robin J. Francis,<sup>†</sup> Andrew Fogg,<sup>†</sup> Dermot O'Hare,<sup>\*,†</sup>  
Nanae Okazaki,<sup>‡</sup> and Kazuyuki Kuroda<sup>‡,§</sup>

*Inorganic Chemistry Laboratory, University of Oxford, South Parks Road,  
Oxford, OX1 3QR, U.K., Department of Applied Chemistry, Waseda University, Ohkubo 3,  
Shinjuku-ku, Tokyo 169, Japan, and Kagami Memorial Laboratory for Materials Science and  
Technology, Waseda University, Nishiwaseda 2, Shinjuku-ku, Tokyo 169, Japan*

*Received January 25, 1999. Revised Manuscript Received April 12, 1999*

In situ, time-resolved energy-dispersive X-ray diffraction has been used to investigate the formation of the mesoporous silicates FSM-16 and MCM-41. The data suggest that the silica-surfactant mesophases formed are highly dependent on the reactant medium, the effect of the silica source being one of the main determining factors. Kanemite, a layered polysilicate, proves to be an excellent silicate source, giving rise to relatively ordered mesophases and subsequent highly ordered mesoporous silicate products. The time-resolved in situ X-ray diffraction data of the kanemite-alkyltrimethylammonium system indicated that the silica-surfactant mesophase precursor to FSM-16 forms from a medium containing a number of intercalated silicate phases, while in contrast, the hexagonal mesophase precursor to MCM-41 forms from a medium containing no other ordered silicate-surfactant phases detectable by in situ X-ray diffraction.

## Introduction

The determination of mechanistic information relating to solid-state reactions should ultimately lead to a more rational approach to the synthesis of microporous and mesoporous materials. Understanding how molecules and ions can preferentially organize themselves under certain conditions to form extended crystalline solid structures is a well-established goal in modern inorganic chemistry. However, it is often difficult to acquire sufficient data to substantiate a particular mechanistic theory that can adequately describe heterogeneous reactions (i.e., involving solid and liquid reagents): Such systems involve a complicated variety of species, nucleation, and crystallization processes. In situ methods can often provide invaluable insights into the nature and the rate of transformation from reactants to products and can therefore shed light on the stages of nucleation and the molecular species involved.<sup>1</sup>

The mechanisms involved in the formation of mesoporous silicates are an important issue in contemporary solid-state chemistry. An additional feature to the problem of examining these reaction mechanisms is that the concept of templating is applied to aggregates, as opposed to single molecules, and involves a variety of inorganic-organic species. Some of the currently reported synthetic routes to silica-surfactant mesophases which are precursors to mesoporous silicates are sum-

marized in Table 1. It appears that there seems to be effectively two independent routes to the synthesis these materials.

The synthetic approach originally reported by Beck, Vartuli, and co-workers<sup>2</sup> led to the development and investigation of the M41S family of mesoporous molecular sieves.<sup>3–6</sup> The three phases obtained from the M41S synthesis methods are hexagonal (MCM-41), cubic (MCM-48), and lamellar (MCM-50), whose microscopy and diffraction data are reminiscent of surfactant/water binary systems. This has led to many extensive in situ NMR studies of the systems,<sup>7–9</sup> and prompted Beck et al. to initially propose a liquid crystal template (LCT) mechanism.<sup>3</sup> Beck et al. describes the process as the formation of liquid crystals by the surfactants, followed by condensation of the silicate framework around the

(2) Kresge, C. T.; Leonowicz, M. E.; Roth, W. J.; Vartuli, J. C.; Beck, J. S. *Nature* **1992**, 359, 710–712.

(3) Beck, J. S.; Vartuli, J. C.; Roth, W. J.; Leonowicz, M. E.; Kresge, C. T.; Schmitt, K. D.; Chu, C. T. W.; Olson, D. H.; Sheppard, E. W.; McCullen, S. B.; Higgins, J. B.; Schlenker, J. L. *J. Am. Chem. Soc.* **1992**, 114, 10834–10843.

(4) Beck, J. S.; Vartuli, J. C.; Kennedy, G. J.; Kresge, C. T.; Roth, W. J.; Schramm, S. E. *Chem. Mater.* **1994**, 6, 1816–1821.

(5) Vartuli, J. C.; Schmitt, K. D.; Kresge, C. T.; Roth, W. J.; Leonowicz, M. E.; McCullen, S. B.; Hellring, S. D.; Beck, J. S.; Schlenker, J. L.; Olson, D. H.; Sheppard, E. W. *Chem. Mater.* **1994**, 6, 2317–2326.

(6) Kresge, C. T.; Vartuli, J. C.; Roth, W. J.; Leonowicz, M. E.; Beck, J. S.; Schmitt, K. D.; Chu, C. T. W.; Olson, D. H.; Sheppard, E. W.; McCullen, S. B.; Higgins, J. B.; Schlenker, J. L. *Stud. Surf. Sci. Catal.* **1995**, 92, 11.

(7) Chen, C.-Y.; Burkett, S. L.; Davis, M. E.; Li, H. X. *Microporous Mater.* **1993**, 2, 27–34.

(8) Steel, A.; Carr, S. W.; Anderson, M. W. *J. Chem. Soc., Chem. Commun.* **1994**, 1571–1572.

(9) Firouzi, A.; Atef, F.; Oertli, A. G.; Stucky, G. D.; Chmelka, B. F. *J. Am. Chem. Soc.* **1997**, 119, 3596–3610.

<sup>†</sup> University of Oxford.

<sup>‡</sup> Department of Applied Chemistry, Waseda University.

<sup>§</sup> Kagami Memorial Laboratory for Materials Science and Technology, Waseda University.

(1) Cheetham, A. K.; Mellor, C. F. *Chem. Mater.* **1997**, 9, 2269–2279.

**Table 1. Summary of Reported Syntheses of Silica–Surfactant Mesophases That Are Precursors to Mesoporous Silicates<sup>a</sup>**

principal investigator	molar gel composition	silicon/surfactant ratio	T (°C)	notes	ref(s)
Beck	1.0 SiO <sub>2</sub> :0.034 Al <sub>2</sub> O <sub>3</sub> : 0.28 C <sub>16</sub> TMACl/OH (30% OH):0.29 TMAOH: 21.2 H <sub>2</sub> O <sup>a</sup>	3.57	150	XRD and TEM show morphology of final product imitates that of surfactant mesophase.	2, 3
Davis	1.0 SiO <sub>2</sub> :0.089 (C <sub>16</sub> TMA) <sub>2</sub> O: 0.154 (TMA) <sub>2</sub> O:0.092 (NH <sub>4</sub> ) <sub>2</sub> O: 0.178 HCl:18.0 H <sub>2</sub> O	5.62	95	<sup>14</sup> N NMR: no H <sub>α</sub> observed in synthesis medium.	7
Anderson	1.0 SiO <sub>2</sub> :0.2 C <sub>16</sub> TMACl: 0.2 TBAOH:20 H <sub>2</sub> O <sup>a</sup>	5.0	90	<sup>14</sup> N NMR: H <sub>α</sub> phase disappears on heating.	8
Stucky	1.0 SiO <sub>2</sub> :0.025 Al <sub>2</sub> O <sub>3</sub> : 0.115 Na <sub>2</sub> O:0.233 C <sub>16</sub> TMACl: 0.089 TMAOH:125 H <sub>2</sub> O	4.29	75	XRD: a layered phase observed or the first ~20 min before a hexagonal phase grows in.	10
Chmelka	1.0 SiO <sub>2</sub> :0.714 TMAOH: 0.357 C <sub>16</sub> TMABr-d <sub>2</sub> :13.4 CH <sub>3</sub> OH: 0.857 TMB:140 H <sub>2</sub> O	2.8	25–60	Lamellar L <sub>α</sub> phase exists at room temperature and can be transformed to a H <sub>α</sub> phase on heating. Process is reversible for these low T, highly alkaline conditions, with strong hysteresis.	9, 12
Kuroda	NaHSi <sub>2</sub> O <sub>5</sub> ·3H <sub>2</sub> O: 0.45 C <sub>16</sub> TMACl:255 H <sub>2</sub> O	1.1	70	Intercalation of the surfactant to form a silicate–organic complex.	16, 17

<sup>a</sup> For convenience of comparison, the compositions have been represented as shown by converting TMA/TBA silicate to SiO<sub>2</sub> and TMA/TBA–OH (assumed ratio of 1:1).

micelles. This mechanistic model served to illustrate the concept of aggregate molecular templating, but was quickly modified to include the role of the silicate anionic species. This model is better described as a process of cooperative assembly, as a result of favorable electrostatic interactions at the inorganic–organic interface.<sup>3,9–12</sup>

Another approach, developed by Kuroda and co-workers, takes advantage of the ability of long-chain alkyltrimethylammonium cations to intercalate into the single-layered polysilicate, kanemite. This was an extension of the intercalation chemistry originally reported by Beneke et al.<sup>13</sup> Kuroda and co-workers initially reported that formation of the silicate–surfactant complex,<sup>14,15</sup> followed by removal of the surfactant led to the formation of a hexagonal mesoporous silicate.<sup>16,17</sup> These materials can be tailor-made with single size distribution channels in the range 20–40 Å. The mesoporous silicate material denoted FSM-16 is produced by intercalation of hexadecyltrimethylammonium cationic surfactants, and the formation process is representative of the transformation of 2D layers to a 3D framework.<sup>18</sup>

FSM-16 is derived by calcination of the silicate–organic complex formed by reaction of hexadecyltrimethylammonium chloride (C<sub>16</sub>H<sub>33</sub>N<sup>+</sup>Me<sub>3</sub>Cl<sup>−</sup> = C<sub>16</sub>–

TMACl) with the single-layer silicate, kanemite (NaHSi<sub>2</sub>O<sub>5</sub>·3H<sub>2</sub>O) at 70 °C. Following calcination the material retains an internal surface area of typically 900 m<sup>2</sup> g<sup>−1</sup> with a narrow pore size distribution.<sup>17</sup> Calcination of the silicate–organic is accompanied with a large shrinkage of the lattice parameter (XRD) that suggests considerable rearrangement of the SiO<sub>4</sub> tetrahedra in the walls of the pores. Solid-state <sup>29</sup>Si MAS NMR of the silicate–organic complex and the final product confirms increased condensation of silanol groups to form siloxane bonds, and distortion of the SiO<sub>4</sub> tetrahedra. X-ray powder diffraction measurements of the silicate–organic complex and FSM-16 show a lattice contraction of 10–20%, depending on calcination temperature.<sup>17,19</sup> The as-synthesized product has been reported to have a wall thickness of 4 Å, which corresponds to sheets of single SiO<sub>4</sub> tetrahedra, resembling kanemite. Calcination causes mass silanol condensation and wrinkling of the silicate sheets to become a double silicate layer of 8–9 Å, closer to wall thicknesses observed for MCM-41. One of the remarkable features of this process is the low concentration of alkyltrimethylammonium (C<sub>n</sub>TMA) cations required, typically 0.1 mol/L (corresponding to about 3.2 wt % for C<sub>16</sub>TMACl) to form the highly ordered mesoporous product. This value is significantly below concentrations necessary for liquid crystal phases and has a Si/Sur ratio lower than for MCM-41 reactions. The mechanism put forward previously by Inagaki et al. is referred to as “folded sheets mechanism” (hence FSM) which involves the collapse and folding of a lamellar material derived from the intercalation of the alkylammonium ions into kanemite.<sup>17,20</sup> Chen et al., studied the differences between MCM-41 and FSM-16 and concluded that kanemite had fragmented to form the organic–inorganic silicate mesophase which is the precursor to FSM-16.<sup>21</sup> We were interested in investi-

(10) Monnier, A.; Schüth, F.; Huo, Q.; Kumar, D.; Margolese, D.; Maxwell, R. S.; Stucky, G. D.; Krishnamurthy, M.; Petroff, P.; Firouzi, A.; Janicke, M.; Chmelka, B. F. *Science* **1993**, *261*, 1299–1303.

(11) Huo, Q. S.; Margolese, D. I.; Ciesla, U.; Feng, P. Y.; Gier, T. E.; Sieger, P.; Leon, R.; Petroff, P. M.; Schüth, F.; Stucky, G. D. *Nature* **1994**, *368*, 317–321.

(12) Firouzi, A.; Kumar, D.; Bull, L. M.; Beiser, T.; Seiger, P.; Huo, Q.; Walker, S. A.; Zasadzinski, J. A.; Glinka, C.; Nicol, J.; Margolese, D.; Stucky, G. D.; Chmelka, B. F. *Science* **1995**, *267*, 1138–1143.

(13) Beneke, K.; Lagaly, G. *Am. Mineral.* **1977**, *62*, 763.

(14) Yanagisawa, T.; Shimizu, T.; Kuroda, K.; Kato, C. *FSM. In 56th National Meeting of the Chemical Society of Japan*, Tokyo; Chemical Society of Japan: Tokyo, 1988; pp Abstr., I, 761, No. IXIID42.

(15) Yanagisawa, T.; Shimizu, T.; Kuroda, K.; Kato, C. *Bull. Chem. Soc. Jpn.* **1990**, *63*, 988–992.

(16) Inagaki, S.; Fukushima, Y.; Kuroda, K. *J. Chem. Soc., Chem. Commun.* **1993**, 680–682.

(17) Inagaki, S.; Koiwai, A.; Suzuki, N.; Fukushima, Y.; Kuroda, K. *Bull. Chem. Soc. Jpn.* **1996**, *69*, 1449–1457.

(18) Schöllhorn, R. *Chem. Mater.* **1996**, *8*, 1747–1757.

(19) Inagaki, S.; Sakamoto, Y.; Fukushima, Y.; Terasaki, O. *Chem. Mater.* **1996**, *8*, 2089–2095.

(20) Inagaki, S.; Fukushima, Y.; Kuroda, K. *Stud. Surf. Sci. Catal.* **1994**, *84*, 125–132.

(21) Chen, C. Y.; Xiao, S. Q.; Davis, M. E. *Microporous Mater.* **1995**, *4*, 1–20.

gating this reaction to gain a conclusive understanding of these processes using time-resolved in situ X-ray diffraction techniques.

The use of in situ energy-dispersive X-ray diffraction (EDXRD) as a technique for monitoring the formation of intercalation compounds and microporous materials is well-established,<sup>22–25</sup> and the literature includes recent reviews on the subject.<sup>1,26</sup> The application of in situ EDXRD to study the formation of mesoporous materials requires monitoring the formation of ordered periodic arrays of aggregate structures at low  $2\theta$ , as opposed to normal crystallization processes. Preliminary investigations of this kind have been performed.<sup>27,28</sup> Here we describe the use of time-resolved in situ energy-dispersive X-ray powder diffraction to investigate the formation mechanism of the hexagonal mesophases derived from kanemite and those that are the precursors to M41S materials.

## Experimental Section

**Reactions.** All surfactants, fumed silica, tetraethyl orthosilicate, and other laboratory reagents were obtained from Aldrich and used as received. Kanemite was prepared from a sodium silicate solution ( $\text{Na}/\text{Si} = 1$ , comprising 15 wt % in water), heated in a platinum crucible from 100 °C to 750 °C at a heating rate of 5 °C/min, and then maintained at 750 °C for 1 h. The product was a  $\delta\text{-Na}_2\text{Si}_2\text{O}_5$ , a bright white solid with a porous appearance. Kanemite (idealized  $\text{NaHSi}_2\text{O}_5 \cdot 3\text{H}_2\text{O}$ ) was made by suspending  $\delta\text{-Na}_2\text{Si}_2\text{O}_5$  (5 g, 27 mmol) in 100 mL of  $\text{H}_2\text{O}$  and stirring at room temperature for exactly 30 min. The timing is crucial for correct exchange of  $\text{Na}^+$  ions for  $\text{H}^+$ . Characterization of both silicates was by XRD, literature values taken.<sup>13,29,30</sup> Solid-state CP MAS  $^{29}\text{Si}$  NMR of Kanemite gave a single isotropic peak at  $-97.0$  ppm ( $\nu_{1/2} = 27.6$  Hz).

The temperature for each in situ diffraction experiment was accurate and stable to  $\pm 1$  °C, and the contents were stirred efficiently with the aid of a magnetic stirrer. The block was preheated for each experiment. For kanemite–surfactant reactions the kanemite/surfactant ratio was 2.2: typically 0.236 g of kanemite (idealized  $\text{NaHSi}_2\text{O}_5 \cdot 3\text{H}_2\text{O}$ ) with a relatively uniform particle size of  $\leq 90$   $\mu\text{m}$  was placed in a Pyrex glass ampule. At the commencement of the reaction, 5 mL 0.1 mol/L  $\text{C}_n\text{TMAX}$  solution ( $n = 12, 14$ ;  $\text{X} = \text{Br}$ ,  $n = 16$ ;  $\text{X} = \text{Cl}$ ) was added and the ampule transferred to the heating block. For MCM-41 reactions, a gel was prepared in a glass ampule suitable for high-pressure reactions and fitted with a greaseless Teflon tap: 0.004 mol  $\text{C}_{16}\text{TMACI}/\text{OH}$  (30% hydroxide, preparation described previously<sup>31a</sup>),  $4.9 \times 10^{-4}$  mol  $\text{Al}_2\text{O}_3$ ,

0.014 mol  $\text{SiO}_2$  (fumed), 0.004 mol tetramethylammonium hydroxide, and 0.1 mol  $\text{H}_2\text{O}$ . The subsequent gel was aged for 1 h prior to placing in the heating block at 150 °C and the ampule sealed. For M41S reactions for which tetraethyl orthosilicate ( $\text{Si}(\text{OEt})_4$ ; TEOS) is the silica source the procedure was followed according to Vartuli et al.<sup>5</sup> involving the combination of  $\text{C}_{16}\text{TMACI}/\text{OH}$  (30% hydroxide) and TEOS in the  $\text{Si}/\text{Sur}$  molar ratios: 0.6 (hexagonal), 1.3 (lamellar).

**Diffraction Experiments.** In situ diffraction studies were performed using the energy dispersive powder diffraction method on Station 16.4 of the U.K. Synchrotron Radiation Source (SRS) at the CLRC Daresbury Laboratory, U.K. The SRS is a low emittance storage ring which runs with an electron beam energy of 2 GeV, ring current approximately 180–250 mA. Station 16.4 is a new white beam facility situated on Beamline 16, where a wiggler magnet of peak field 6 T is located. It receives useful X-ray flux in the range 5 to 140 keV, with a maximum intensity at about 20 keV. The position of the maximum intensity at the detector is shifted to higher energy on introduction of the experimental apparatus, due to the absorption of lower energy photons by the cell. Useful intensity could be obtained above about 20 keV using Pyrex glassware with a peak flux of approximately  $7 \times 10^{11}$  photons  $\text{s}^{-1} \text{mm}^2$  in a 0.1% bandwidth at 10 keV. The radiation from the synchrotron passed through a collimator on to the sample and diffracted X-rays passed through a set of post sample slits and into the detector. The detector is an intrinsic germanium crystal which counts the number of incident photons that enter it and determines their energy. The detector momentum resolution ( $\Delta E/E = 0.0253$ ) is increased by the postsample molybdenum slits to ( $\Delta E/E = 0.0115$ ).

The sample size of the diffraction apparatus used might be expected to lead to significant peak broadening. However, the use of the long postsample collimation and energy dispersive technique allows a large diffraction “lozenge” without the sample size significantly affecting resolution (Figure 1). A more detailed technical description of the apparatus used in these experiments has been given elsewhere.<sup>32,33</sup> The precise form of the energy profile  $I(E)$  is complex and varies from reaction to reaction. The broad backgrounds observed in the energy-dispersive X-ray diffraction (EDXRD) spectra is due to diffuse scatter from the cell materials, sample, and solvent. Figure 1 shows a schematic diagram of the experimental setup used for all the experiments.

XRD was used to characterize powder samples, including the mesoporous silicates obtained from the reactions. Following workup, X-ray powder patterns of the samples were recorded on a Siemens D5000 diffractometer. Monochromatic  $\text{Cu K}\alpha_1$  radiation ( $\lambda = 1.54056$  Å) at 40 kV and 30 mA was used.

**Data Collection.** The energy [ $E$  (keV)] at which a Bragg peak corresponding to a particular interplanar spacing [ $d$  (Å)] occurs in the EDXRD spectrum is given by

$$E = 6.19926/(d \sin \theta) \quad (1)$$

where  $\theta$  is the diffraction angle in degrees (Figure 1). In the experiments reported here we typically choose a fixed diffraction angle of  $0.7^\circ$  ( $2\theta$ ) so that Bragg reflections with  $d$  spacings  $\sim 30$  Å occurred at  $\sim 40$  keV, close to the maximum in the transmission spectrum of these samples. This geometrical setting allows the detector to sample a useable energy range equivalent to a  $d$  spacing range of approximately 40–13 Å. For such low-angle (high  $d$  spacing) data collection, it is anticipated that X-ray scattering will give rise to relatively broad peaks. By differentiating eq 1 with respect to  $d$ , it is

(22) Evans, J. S. O.; Francis, R. J.; O'Hare, D.; Price, S. J.; Clark, S. M.; Flaherty, J.; Gordon, J.; Nield, A.; Tang, C. C. *Rev. Sci. Instrum.* **1995**, *66*, 2442.

(23) Francis, R. J.; Price, S. J.; Evans, J. S. O.; O'Brien, S.; O'Hare, D. *Chem. Mater.* **1996**, *8*, 2102–2108.

(24) Evans, J. S. O.; Price, S. J.; Wong, H.-V.; O'Hare, D. *J. Am. Chem. Soc.* **1998**, *120*, 10837.

(25) Francis, R. J.; O'Brien, S.; Fogg, A. M.; Halasyamani, P. S.; O'Hare, D.; Louiseau, T.; Férey, G. *J. Am. Chem. Soc.* **1999**, *121*, 1002.

(26) Francis, R. J.; O'Hare, D. *J. Chem. Soc., Dalton Trans.* **1998**, 3133–3148.

(27) O'Brien, S.; Francis, R. J.; Price, S. J.; O'Hare, D.; Clark, S. M.; Okazaki, N.; Kuroda, K. *J. Chem. Soc. Chem. Commun.* **1995**, 2423–2424.

(28) Linden, M.; Schunk, S. A.; Schüth, F. *Angew. Chem., Int. Ed. Engl.* **1998**, *37*, 821.

(29) Williamson, J.; P., G. F. *Phys. Chem. Glasses* **1966**, *7*, 127–138.

(30) Johan, Z.; Maglione, G. F. *Bull. Soc. Fr. Mineral. Cristallogr.* **1972**, *95*, 371–382.

(31) (a) O'Brien, S.; Keates, J. M.; Barlow, S.; Drewitt, M. J.; Payne, B. R.; O'Hare, D. *Chem. Mater.* **1998**, *10*, 4088–4099. (b) Mesophase is the term commonly used to describe the intermediate inorganic–surfactant assembly.

(32) Clark, S. M.; Irvin, P.; Flaherty, J.; Rathbone, T.; Wong, H. V.; Evans, J. S. O.; O'Hare, D. *Rev. Sci. Instrum.* **1994**, *65*, 2210. Clark, S. M.; Cernik, R. J.; Grant, A.; York, S.; Atkinson, P. A.; Gallagher, A.; Stokes, D. G.; Gregory, S. R.; Harris, N.; Smith, W.; Hancock, M.; Miller, M. C.; Ackroyd, K.; Farrow, R.; Francis, R.; O'Hare, D. *Mater. Sci. Forum* **1996**, *228*, 213–217.

(33) Clark, S. M.; Evans, J. S. O.; O'Hare, D.; Nuttall, C. J.; Wong, H. V. *J. Chem. Soc., Chem. Commun.* **1994**, 809–810.



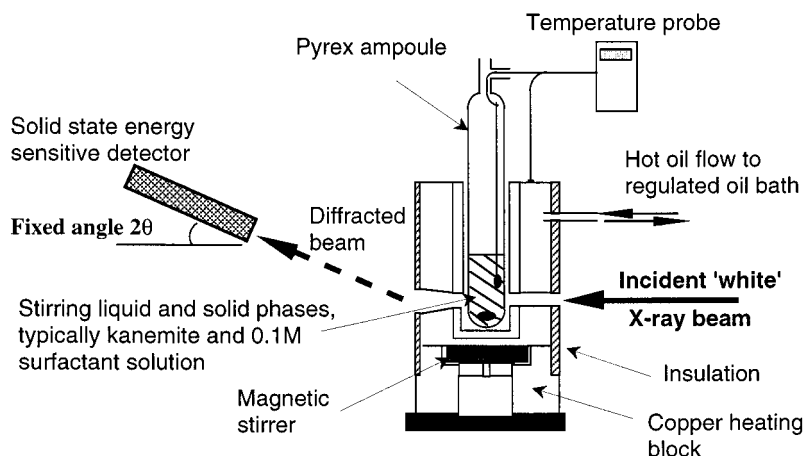


**Figure 1.** Schematic diagram of the experimental cell used to record time-resolved in situ energy dispersive powder X-ray diffraction data on Station 16.4 at the SRS, Daresbury Laboratory, U.K.

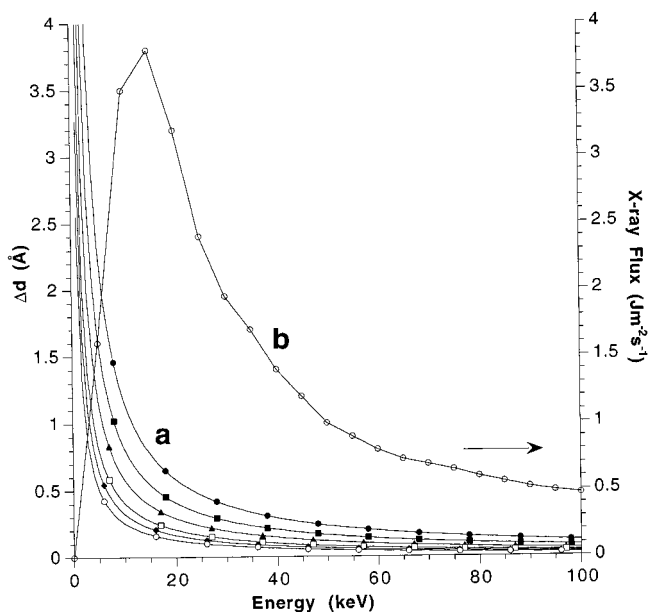


**Figure 2.** (a) Calculated  $\Delta d$  curves ( $\text{\AA}$ ) for the energy discriminating detector in the energy range 0–80 keV for a range of fixed detector angles ( $2\theta$ , see Figure 1) ( $\bullet = 0.35^\circ$ ,  $\blacksquare = 0.5^\circ$ ,  $\blacktriangle = 0.7^\circ$ ,  $\square = 1.0^\circ$ ,  $\blacklozenge = 1.25^\circ$ ,  $\circ = 1.6^\circ$ ) and (b) the incident X-ray flux ( $\phi$ ) as a function of energy for a  $1.6^\circ$  detector angle.

possible to show that the magnitude of detector resolution,  $\Delta E/E$ , is equal to  $\Delta d/d$ :

$$\partial E/\partial d = -6.199\,26/(d^2 \sin \theta) \quad (2)$$

Substituting  $E = 6.199\,26/(d \sin \theta)$

$$\Delta E = -E(\Delta d/d) \quad (3)$$

Since the magnitude of  $\Delta E/E = 0.0115$ , at detector angles at around  $0.7^\circ$  ( $2\theta$ ), it is calculated that peak resolution due to the detector alone will be  $0.5\text{--}0.3\text{ \AA}$  over the 20–40 keV range. By calculating  $(\Delta E d)/E$  for a series of detector angles, it is possible to obtain an expected estimate of the resolution in  $d$  spacing, or  $\Delta d$ , over the energy dispersive range. Combined with the flux of the energy-dispersive X-rays, the “ $\Delta d$  curves” provide a means of determining the energy range appropriate for peak resolution, shown in Figure 2.

**Data Analysis.** Integrated intensities of all the signals in the EDXRD spectra were calculated by an automated Gaussian curve fitting routine. It is sometimes convenient to convert the experimental integrated intensity data to the dimension-

less quantity termed the extent of reaction ( $\alpha$ ). The value of  $\alpha$  at any time ( $t$ ) for the growth of a new crystalline phase is defined by

$$\alpha_{\text{intercalate}}(t) = [I_{hkl}(t)]/[I_{hkl}(t_\infty)] \quad (4)$$

where  $I_{hkl}(t)$  represents the integrated intensity of a reflection ( $hkl$ ) at time  $t$ , and  $I_{hkl}(t_\infty)$  is the integrated intensity when the reaction is complete. In addition, the decay of a crystalline phase can also be followed using eq 5:

$$\alpha_{\text{host}}(t) = 1 - [I_{hkl}(t)]/[I_{hkl}(t_0)] \quad (5)$$

where  $I_{hkl}(t)$  represents the integrated intensity of the Bragg reflection ( $hkl$ ) at time  $t$ , and  $I_{hkl}(t_0)$  is the initial intensity of that reflection.

## Results and Discussion

**In Situ Study of the Formation of Silica-Surfactant Mesophases<sup>31a</sup> Derived from Kanemite.** We have recorded time-resolved in situ energy-dispersive X-ray powder diffraction (EDXRD) spectra following the addition of an aqueous solution of hexadecyltrimethylammonium chloride ( $\text{C}_{16}\text{H}_{33}\text{N}^+\text{Me}_3\text{Cl}^- = \text{C}_{16}\text{TMACl}$ ) to kanemite at  $70^\circ\text{C}$  over a period of 3 h. The spectra are shown accumulated as a three-dimensional stacked plot in Figure 3a, along with the final spectrum recorded after 276 min (Figure 3b) which clearly indicate the diffraction peaks present.

The stacked and single spectra can be described as a series of broad Bragg reflections viewed in energy space that arise due to the growth of “crystalline” silica-surfactant mesophases from the medium. A stirred suspension of kanemite at this pH and temperature showed only a broad featureless background, thus overwhelming X-ray scattering due to the silicate particles can be ruled out. We expect the coherent X-ray scattering at these low angles (high  $d$  spacing) to produce broad Bragg reflections due to the convolution of the small ordered domain size of the silica-surfactant mesophases and the resolution function of the diffractometer setup.

Following the addition of the 0.1 M solution of  $\text{C}_{16}\text{TMACl}$ , a Bragg reflection grows in at a  $d$  spacing of  $\sim 32\text{ \AA}$  within 10 min. The  $d$  spacing of this reflection increases gradually throughout the course of the reaction reaching a constant value of  $33.2\text{ \AA}$  after 30 min.

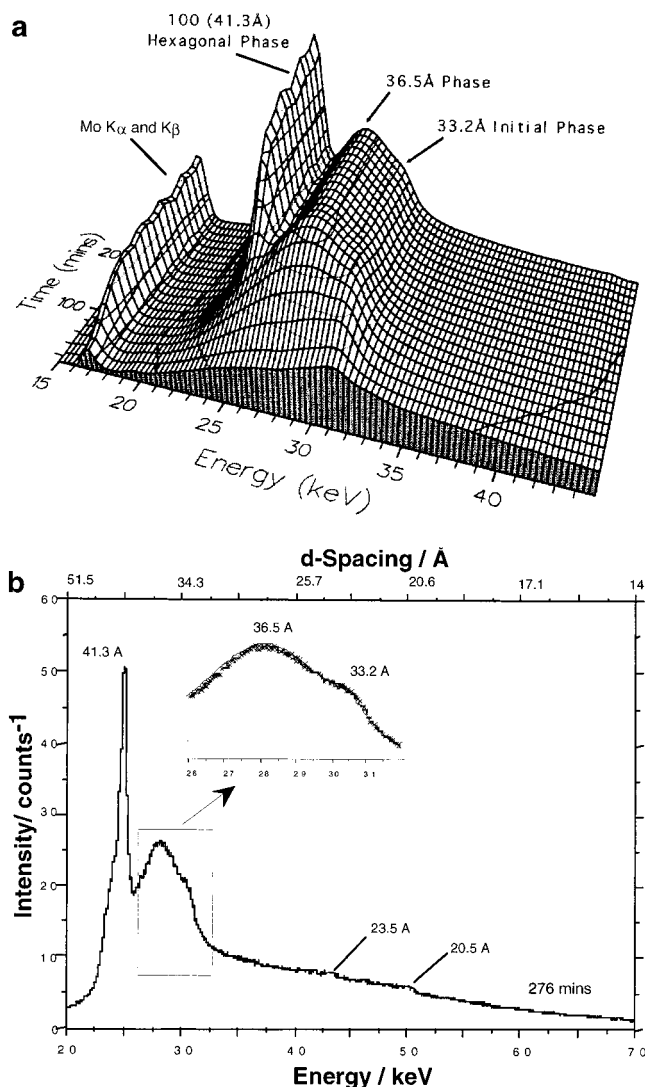


**Figure 3.** (a) Three-dimensional stacked plot showing the energy dispersive powder X-ray diffraction spectra recorded following addition of 0.1 M hexadecyltrimethylammonium chloride ( $C_{16}TMA^+Cl^-$ ) to kanemite in water at 70 °C and (b) the final in situ EDXRD spectrum taken after reaction completion, showing all observable diffraction features.

Subsequently, a second even broader Bragg reflection grows in with a  $d$  spacing of  $\sim 36$  Å reaching a maximum after  $\sim 100$  min. Once this Bragg reflection has reached its maximum intensity, we observed the growth of a series of reflections at  $d$  spacings of 41.3, 23.5, and 20.5 Å. These reflections can be indexed as the (100), (110), and (200) Bragg reflections corresponding to a hexagonal symmetry mesophase ( $a = 47.7$  Å,  $2d_{100}/\sqrt{3}$ , see Figure 3). After pH adjustment with HCl to 8.5 to promote silanol condensation, filtration, and calcination, FSM-16 is formed. The in situ diffraction data shown in Figure 3 clearly shows that the hexagonal (41 Å) silica mesophase forms before dissolution of all the crystalline silicates.

It is highly likely that the intermediate phase with  $d$  spacing of 33.2 Å has a layered, two-dimensional structure. A series of 00/ reflections with  $c$  lattice constant of 30.5 Å was observed in the laboratory X-ray powder diffraction pattern together with the Bragg reflections of the hexagonal phase from the untreated filtrate isolated after the reaction (Figure 4). It is

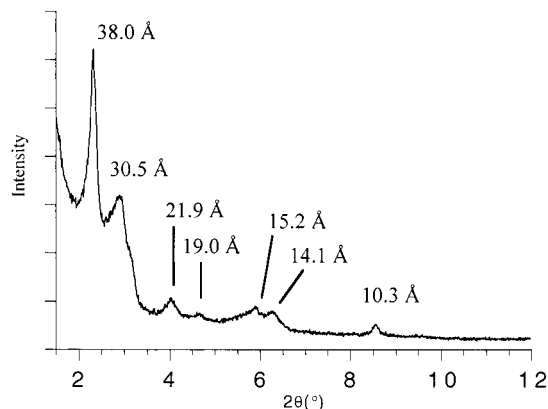


**Figure 4.** X-ray powder diffraction pattern of the filtrate recovered from an in situ reaction, after 0.1 M hexadecyltrimethylammonium chloride was reacted with kanemite (kanemite/ $C_{16}TMA = 2.2$ ) at 70 °C for 4 h.

reasonable to assume that the 00/ reflections belong to the lamellar phase observed by in situ EDXRD, and the increased  $d$  spacing of the 001 reflection is due to swelling in the reaction medium. This has been observed in the intercalation chemistry of kanemite.<sup>34a</sup> An interlayer separation of  $\sim 30$  Å is consistent with intercalated  $C_{16}TMA^+$  ions with an estimated length of  $\sim 23$  Å,<sup>34b</sup> and a silicate layer of  $\sim 6$  Å. Lamellar phases appear to be common to all kanemite-surfactant reactions regardless of chain length (see also Table 3 and relevant discussion below). Recovery of this lamellar phase from the reaction mixture is possible by filtering the product before the reaction is complete and prior to addition of 1.0 M HCl. However, calcination of this sample led to a condensed amorphous phase, and collapse of any porous structure.

The structure of the material responsible for the broad reflection (fwhm of  $\sim 4$  keV,  $\sim 6$  Å) centered at  $d$  spacing = 36.4 Å is unknown, and cannot be observed in the powder diffraction pattern of the solid products recovered by filtration (Figure 4). The phase is therefore not sufficiently condensed to completely survive recovery to a solid product. We believe this second Bragg reflection can be assigned to a partially ordered silica-surfactant mesophase, hereafter described as the POSSM phase. The broadness of the reflection and lower intensity of the X-ray scattering suggest that the POSSM phase occurs due to the ordering of fragmented anionic silicate layers and cationic surfactant molecules. The EDXRD profile is similar to that of the dilute, weakly assembled M41S species shown later in Figure 10. Furthermore the phase persists at higher temperatures and eventually dominates over the sharp  $\sim 40$  Å hexagonal mesophase. In the same cetyltrimethylammonium-kanemite reaction at 104 °C (Figure 6), kanemite fully dissolves, and the broad phase is still observed by EDXRD. It could therefore be described as a liquid crystal mesophase present in the solution, as a result of silicate species and surfactant assemblies. Such an explanation would account for the time taken for the POSSM phase to appear (due to slow, partial dissolution of kanemite), and for the loss of this phase following

(34) (a) Kuroda, K. Unpublished results, 1997. (b) The parallel interatomic distance between two carbons is 1.27 Å, and the headgroup,  $\sim 3$  Å:  $(16 \times 1.27) + 3 = 23.3$  Å.

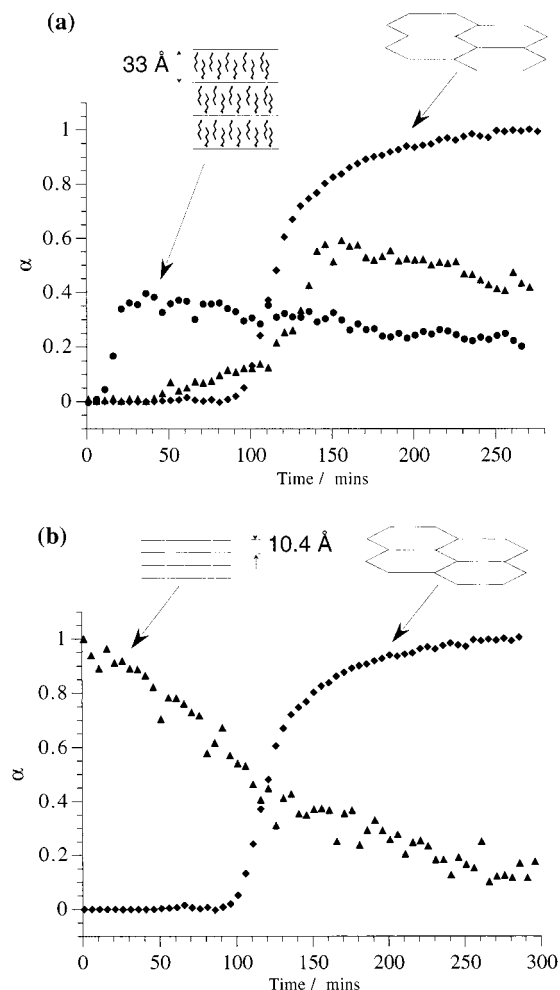


**Figure 5.** (a) Plot of extent of reaction ( $\alpha$ ) vs time for each order phase formed by the reaction of 0.1 M  $C_{16}$ TMACl with kanemite in water at 70 °C: (◆) 100 Bragg reflection of the hexagonal phase; (●) intermediate phases at  $d = 33$  Å; and (▲) POSSM phase at  $d = 36$  Å. Note: the intensities were scaled to the maximum intensity of the 100 Bragg reflection of the hexagonal phase for size comparison. (b) The evolution of the 100 Bragg reflection of the hexagonal phase (◆) and concurrent decay of 100 Bragg reflection of kanemite (▲,  $d = 10.4$  Å).

recovery of the solid products by filtration. The POSSM phase appears to be present in all kanemite-alkyltrimethylammonium intercalation reactions studied by in situ EDXRD, regardless of chain length. It is therefore likely that the POSSM phase contributes to the formation of the silicate-organic complex formed following pH adjustment that, when calcined, produces a hexagonal mesoporous silicate.

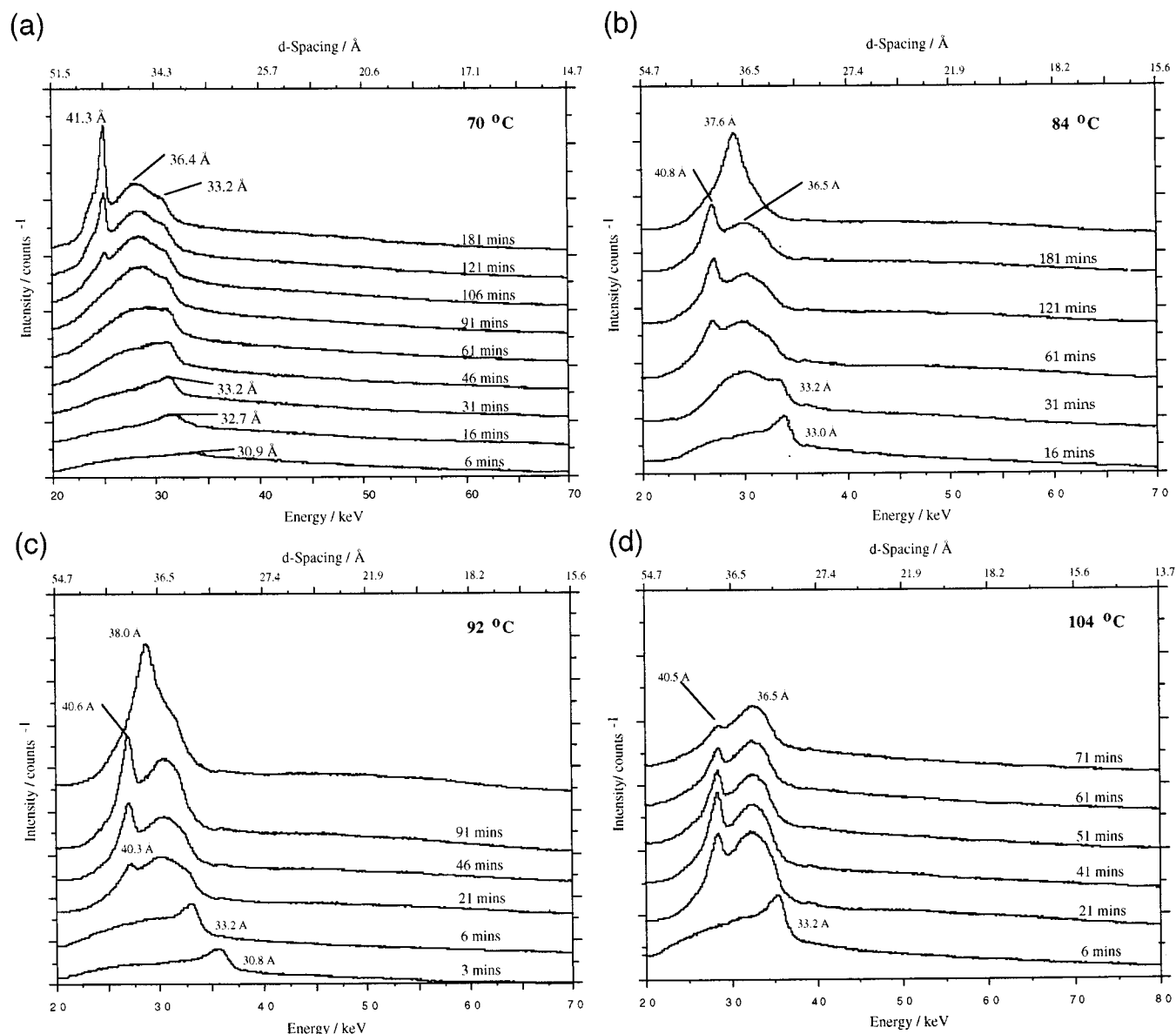
Integration of the intensities of the reflections observed by in situ EDXRD are shown in Figure 5. A decrease in the integrated intensities of both the lamellar phase at 33.2 Å and the POSSM phase can be observed following the onset of the hexagonal mesophase ( $a = 47.7$  Å). The decrease of the integrated intensity of the 001 Bragg reflection of the lamellar phase suggests that to some extent, there is a continuous lamellar to hexagonal-phase conversion. This is consistent with the notion of transformation of silicate sheets to a three-dimensional hexagonal array. The evolution of the integrated intensity of the 100 Bragg reflection of the hexagonal phase and concomitant decay

of kanemite 001 Bragg reflection at  $d = 10.4$  Å is also shown in Figure 5b. It was necessary to monitor the decay of crystalline kanemite independently by adjusting the detector to a higher angle to receive sufficient beam flux. Comparison with the decay of kanemite  $d_{001}$  in pure water indicated that the influence of the surfactant is to rapidly accelerate the consumption of kanemite. This observation illustrates the role of the cationic surfactant both in intercalation and distortion of the silicate sheets, which serve to disrupt the layered periodicity of kanemite. A small quantity (5–10%) persists after the formation of the hexagonal mesophase, demonstrating the ability of some of the layered polysilicate to remain intact under these conditions. It is known that the nature of the wall of the final product, FSM-16, is different to the silicate sheets of kanemite, and that considerable structural rearrangement of the silicate sheets occurs even prior to calcination.<sup>35</sup> The in situ EDXRD observations support the proposal that the hexagonal phase isolated from the reaction medium is derived from these kanemite sheets.

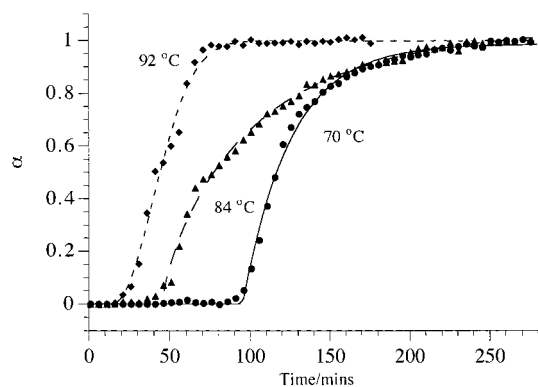
**Effect of Temperature.** To investigate the effect of temperature on the formation of silica-surfactant phases derived from kanemite, in situ EDXRD data were recorded by following the addition of a 0.1 M aqueous solutions of  $C_{16}$ TMACl to a suspension of kanemite (kanemite/ $C_{16}$ TMACl = 2.2) in the temperature range 50–110 °C. In the temperature range 70–110 °C, the growth of three distinct, ordered phases were observed. A series of individual spectra depicting phase evolution over time for a range of temperatures is shown in Figure 6. Extent of reaction ( $\alpha$ ) vs time ( $t$ ) plots based on the integral of the intensity of the 100 Bragg reflection Bragg reflection of the hexagonal phase at temperatures 70, 84, and 92 °C are shown in Figure 7.

Table 2 summarizes the results obtained from these experiments. As expected, there is a marked decrease in induction time with increasing temperature. The rate of growth of the 100 Bragg reflection of the hexagonal phase also increases, but reaches a plateau of lower intensity than compared to that formed at 70 °C. At 84 and 92 °C, the integrated intensity of the 100 Bragg reflection was ~40% of that recorded for the identical experiment performed at 70 °C. Although caution is necessary when comparing the absolute intensities of the 100 Bragg reflection between experiments, this observation is reproducible, taking into account variation in the incident beam intensity between experiments. These observations suggest 70 °C is optimal for the formation of the most highly ordered mesoporous silicate. We believe the intercalation of surfactant molecules into kanemite is maximized at this temperature without significant dissolution of the silicate host. The formation of the hexagonal phase in situ, prior to acidification of the mixture is crucial to the formation of a highly ordered hexagonal silicate-organic phase. Increasing the temperature to 104 °C in a sealed ampule (hydrothermal conditions) promotes the full conversion of kanemite into dissolved silicate species (Figure 6d), with a concurrent increase in pH (initial pH of suspension = 10.5; final pH clear solution = 12.5). Under these

(35) Sakamoto, Y.; Inagaki, S.; Ohsuna, T.; Ohnishi, N.; Fukushima, Y.; Nozue, Y.; Terasaki, O. *Microporous Mesoporous Mater.* **1998**, *21*, 589–596.



**Figure 6.** Stack plots of EDXRD spectra recorded for the reaction of 0.1 M  $C_{16}TMACl$  with kanemite in water at a range of temperatures; (a) 70 °C, (b) 84 °C (c) 92 °C, and (d) 104 °C. In the case of b and c the subsequent pH reduction to 8.5 after reaction completion is also shown.



**Figure 7.** Plot of extent of reaction ( $\alpha$ ) vs time for the reaction of 0.1 M  $C_{16}TMACl$  with kanemite in water at a range of temperatures: 70 °C (●); 84 °C (◆); and 92 °C (▲). Note: the intensities were scaled to the maximum intensity of the 100 Bragg reflection of the hexagonal phase for comparison.

conditions a solid hexagonal phase is unable to form for this silicate/surfactant ratio. The POSSM phase persists

**Table 2. Summary of the Effects of Temperature on the Reaction of Kanemite with  $C_{16}TMACl$ <sup>a</sup>**

$T$ (°C)	$t_0^b$ (min)	$t_{com}^c$ (min)	$d_{100}$ (Å) of hex phase from EDXRD	observations from EDXRD and comments on calcined products, determined by XRD
50	—	—	—	broad, poorly ordered phase
60	—	—	—	broad, poorly ordered phase
70	95	241	41.3	highly ordered mesoporous silicate
84	45	211	40.8	poorly defined mesoporous silicate
92	15	91	40.3	poorly defined mesoporous silicate
104	11	N/A	40.5	clear solution obtained

<sup>a</sup> Kanemite: $C_{16}TMACl$  ratio = 2.2. <sup>b</sup>  $t_0$  = induction time for the growth of the ordered hexagonal phase. <sup>c</sup>  $t_{com}$  = time for completion of growth of  $d_{100}$  (ordered hexagonal phase).

however, providing further evidence that X-ray scattering at this  $d$  spacing can be ascribed to a dissolved, liquid crystal silicate–surfactant phase. The phase may be similar in nature to the hexagonal phase observed



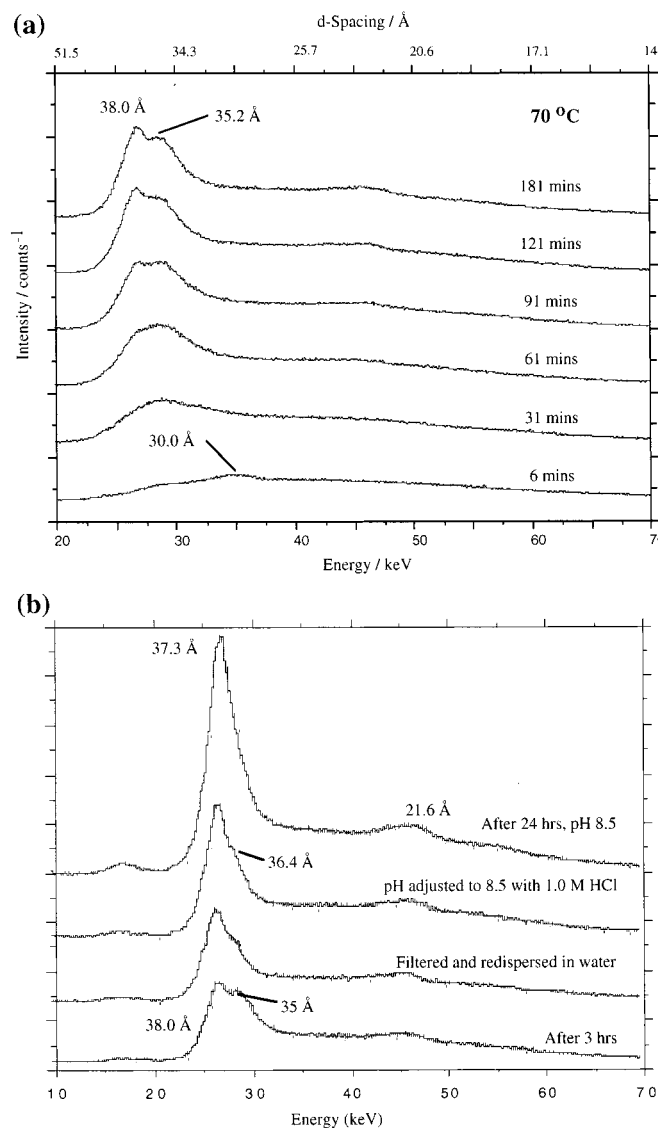


**Figure 8.** (a) Stack plots of in situ EDXRD spectra recorded for the reaction of 0.1 M  $C_{14}$ TMACl with kanemite in water at 70 °C and (b) in situ EDXRD spectra of kanemite/ $C_{14}$ -TMABr, after heating for 3 h at 70 °C. The spectra were taken before and after filtering and after redispersion in water, and after pH adjustment using 1.0 M HCl.

by SAXS in previously reported alkaline conditions favorable for lyotropic silicate-surfactant liquid crystals.<sup>9</sup>

**Addition of HCl—Silanol Condensation.** The addition of 1.0 M HCl is a necessary step in the synthesis of a highly ordered mesoporous silicate derived from kanemite. A pH of 8–9 is known to be favorable for the precipitation of silica from aqueous solution.<sup>36</sup> A reduction of the pH from 12.5 to 8.5 by addition of 1.0–2.0 M HCl to the product mixture immediately causes a striking change in the in situ diffraction pattern (Figure 6b,c). The in situ time-resolved EDXRD spectra of the reaction of 0.1M  $C_{14}$ TMA with kanemite (kanemite/ $C_{14}$ -TMA = 2.2) over a 3-h period is shown in Figure 8a. The 100 Bragg reflection of the hexagonal phase is less prominent than for the  $C_{16}$ TMA/kanemite reaction, but

still clearly visible. Figure 8b shows the effect of each stage in the laboratory work up of the silicate-organic complex obtained from the reaction of 0.1 M  $C_{14}$ TMABr with kanemite, and is typical for the  $C_n$ TMA/kanemite system. Removal of the dissolved species by both decantation and filtration followed by dispersion in water and adjustment to pH 8.5 results in the broadening and growth, especially after 24 h, of the hexagonal phase 100 Bragg reflection. For  $C_n$ TMA/kanemite reactions ( $n = 14, 16$ ), the products recovered by filtration were confirmed by XRD to be hexagonal phases which can be calcined to produce a highly ordered mesoporous silicate. Combined with evidence from the solid-state  $^{29}\text{Si}$  NMR of increased  $Q_4$  units,<sup>17</sup> it can be concluded that condensation of silanol groups to form siloxane bonds occurs during pH adjustment. However, there is no further evidence from the in situ EDXRD data for the persistence of a 33 Å lamellar phase, the remainder of which is presumably converted to the hexagonal phase.

**Role of the Surfactant Chain Length and Concentration.** We have performed a series of in situ EDXRD experiments to study the effect of altering the surfactant type and concentration on the formation of hexagonal mesophases derived from kanemite. A variety of different cationic alkyltrimethylammonium surfactants and a range of concentrations were investigated. Significant results are summarized in Table 3.

With the use of a standard 0.1 M concentration of surfactant, our in situ experiments show that  $C_{16}$ TMACl is the optimal template for the formation of the most highly ordered hexagonal mesoporous materials. Following pH adjustment and calcination, samples with  $n = 16$  tended to exhibit the highest degree of pore regularity, on the basis of powder XRD analysis and consistent with previously published diffraction data.<sup>17</sup> Assuming that the driving force for the formation of the hexagonal phase is partly due to aggregation of the surfactant molecules, a surfactant with a higher tendency to form cylindrical micelles may improve the degree of pore regularity of the product. For example,  $C_{12}$ TMA ions do not form cylindrical micelles<sup>37</sup> which may explain why only an intermediate lamellar phase ( $d = 36$  Å) is attained. The degree of dissociation between the cationic headgroup of the surfactant and the halide anion may account for the differing behavior of the alkyltrimethylammonium/kanemite intercalates. For example, the chloride salt may exchange  $C_{16}\text{TMA}^+$  ions for  $\text{Na}^+$  more readily than for the bromide analogue which could explain why a less defined hexagonal phase is observed by in situ EDXRD. The sensitivity of the intercalation reaction to the concentration of the surfactant is also demonstrated by observing the reaction at half-concentration (Table 3). The ordered hexagonal phase did not form, indicating that the conditions are undesirable for the preparation of FSM silicates at this Si/Surfactant ratio. The delicate thermodynamic balance involved among the surfactant, the dissolved silicate species, and the polysilicate layers must be responsible for this effect.

(36) Iler, R. K. *The Chemistry of Silica*; J. Wiley and Sons, Inc.: New York, 1979; p 46.

(37) Huo, Q. S.; Margolese, D. I.; Ciesla, U.; Demuth, D. G.; Feng, P. Y.; Gier, T. E.; Sieger, P.; Firouzi, A.; Chmelka, B. F.; Schüth, F.; Stucky, G. D. *Chem. Mater.* **1994**, *6*, 1176–1191.

**Table 3. Summary of the in Situ EDXRD Studies Showing the Effect of Surfactant Type on the Kanemite–Surfactant System**

surfactant <sup>a</sup>	silicon/surfactant ratio	observations from EDXRD	<i>t</i> <sub>com</sub> <sup>b</sup> (h)
C <sub>16</sub> TMA <sup>+</sup> Cl <sup>−</sup>	1.1	formation of hexagonal phase (see text)	3
C <sub>16</sub> TMA <sup>+</sup> Cl <sup>−</sup>	0.55	A 33.2 Å lamellar phase grows in over ~10–30 min with concurrent growth of 36 Å phase. No hexagonal phase observed.	2
C <sub>14</sub> TMA <sup>+</sup> Br <sup>−</sup>	1.1	Growth and rapid disappearance of lamellar phase at 29 Å, growth of 35 Å phase and hexagonal phase, <i>d</i> <sub>100</sub> = 38 Å.	1
C <sub>16</sub> TMA <sup>+</sup> Br <sup>−</sup>	1.1	Broad hexagonal phase, <i>d</i> <sub>100</sub> = 37.2 Å.	2
C <sub>18</sub> TMA <sup>+</sup> Br <sup>−</sup>	1.1	Broad hexagonal phase, <i>d</i> <sub>100</sub> = 38.9 Å.	2
C <sub>12</sub> TMA <sup>+</sup> Br <sup>−</sup>	1.1	Broad phase at 34 Å appears but no further phase ordering occurs.	2

<sup>a</sup> For all reactions temperature was maintained at 70 °C. <sup>b</sup> *t*<sub>com</sub> = time to completion of reaction, the point at which the product phase *d*<sub>100</sub> reaches maximum intensity.

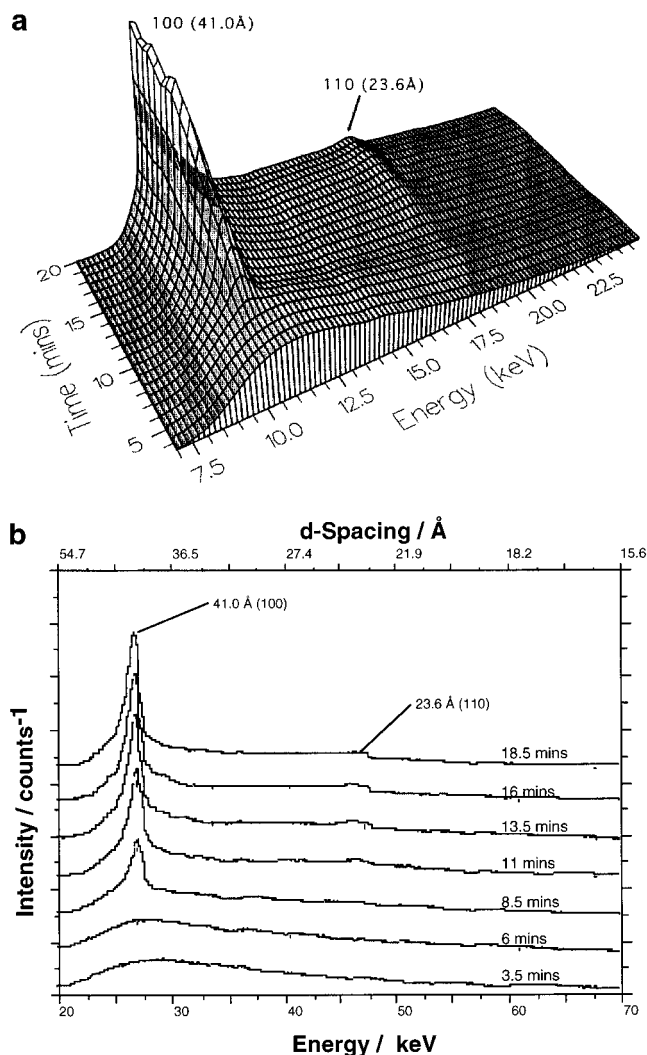


**Figure 9.** (a) Three-dimensional stacked plot of the time resolved, in situ energy-dispersive X-ray diffraction spectra of the gel leading to the formation of the silicate-surfactant precursor to MCM-41 at 150 °C in a sealed ampule, and (b) stacked plot of some of the initial EDXRD spectra showing the rapid growth of the hexagonal phase.

**In Situ Study of the Formation of Silica–Surfactant Precursors to MCM-41.** Recent developments have clarified that molecular assemblies of surfactants can work as templates for the preparation of inorganic–organic mesophase materials which yield highly ordered mesoporous materials such as the M41S family including hexagonal MCM-41. Figure 9 shows the time-resolved in situ energy-dispersive X-ray powder diffrac-

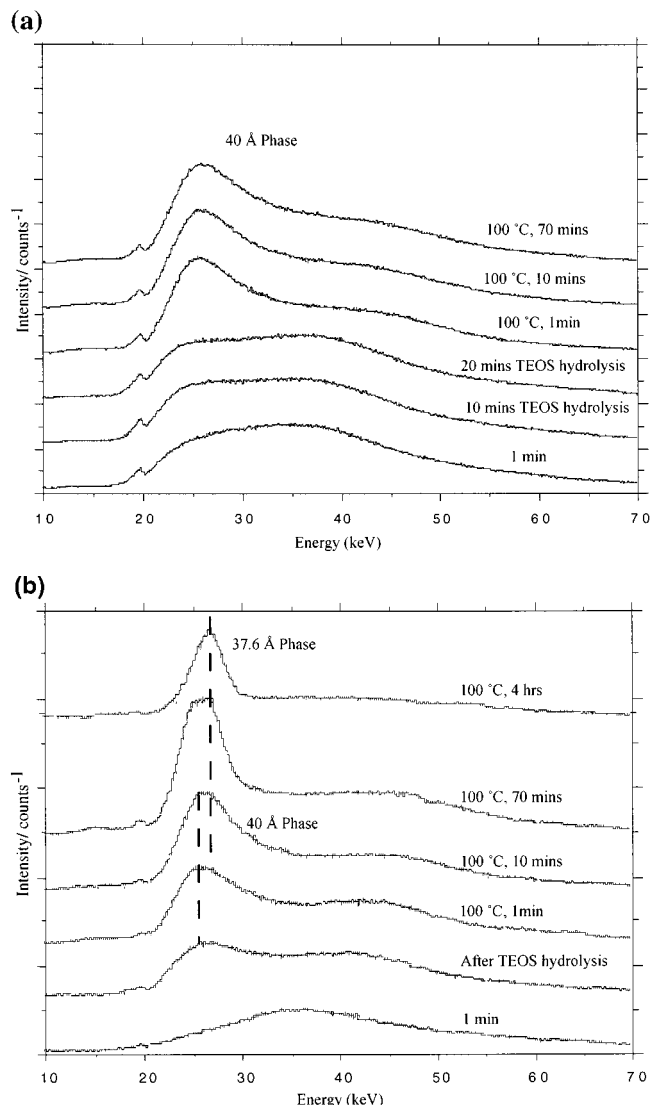
tion data for the synthesis of silica-surfactant mesophase which on calcination yields MCM-41 using the conditions described by Kresge et al.<sup>2</sup> The diffraction data shows the smooth growth of the intensity of the (100) and (110) Bragg reflections of the silica-surfactant hexagonal mesophase precursor to MCM-41; no peaks assignable to any intermediate crystalline silicates are observed. These data are consistent with the results reported by Chen et al.,<sup>21</sup> in which <sup>14</sup>N NMR spectroscopy provided evidence that no liquid crystal phases were formed by the surfactant prior to the formation of the silicate-surfactant mesophase, and no other phases were observed in the synthesis medium. The mechanism originally proposed by Monnier et al.<sup>10</sup> involved an initial lamellar to hexagonal phase transition. This process was not observed here, suggesting that this model does not strictly apply to the preparation of MCM-41, although this phenomenon can be observed under reversible conditions.<sup>9</sup> Further experiments of MCM-41 type syntheses were monitored by the in situ EDXRD technique, using a pre-prepared gel of composition 1.0 SiO<sub>2</sub>:0.025 Al<sub>2</sub>O<sub>3</sub>:0.115 Na<sub>2</sub>O:0.233 C<sub>16</sub>TMACl:0.089 TMAOH:125 H<sub>2</sub>O, at 65 and 75 °C. At both temperatures the formation of a hexagonal phase at ~41 Å was only observed.

A series of experiments using a 29 wt % solution of C<sub>16</sub>TMA Cl/OH (30% exchanged OH) and tetraethyl orthosilicate (TEOS) were performed and monitored by in situ EDXRD and the observations are described in Table 4. Increasing the Si/Sur ratio permits a route to obtaining different products belonging to the M41S family of molecular sieves.<sup>5</sup> In the original MCM-41 synthesis reaction, the mixture is a thick gel prior to reaction. The heat and pressure cause the almost immediate precipitation of the silicate–organic complex in bulk. The conditions for the formation of M41S silicates, using TEOS as the source, are milder which allows an even suspension to be stirred in the synchrotron beam. EDXRD spectra of these suspensions repeatedly showed the formation of very broad phases after the hydrolysis of TEOS. The stack plots featured in Figure 10 describe the reactions for Si/Sur = 0.6 (a) and 1.3 (b), ratios appropriate for the formation of the hexagonal and lamellar phases, respectively. The single broad peaks that appeared (fwhm up to 8 Å) were assigned to be precursor phases to the formation of ordered mesoporous M41S materials. The first spectra show there is negligible scattering prior to hydrolysis.

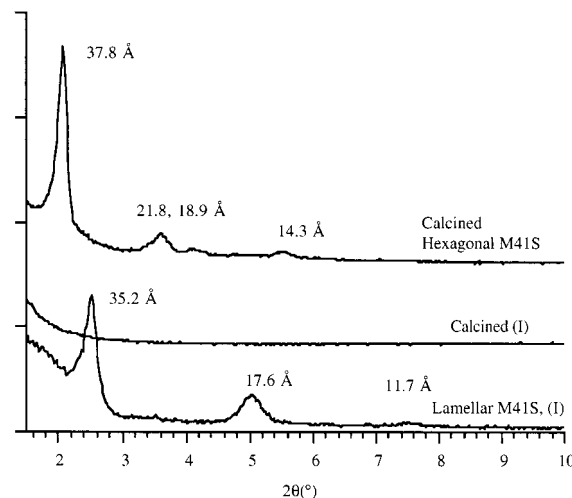
In both cases a 40 Å phase, assigned to be the hexagonal phase, is observed by in situ EDXRD and was typical for all TEOS-surfactant reactions. X-ray powder

**Table 4. Table of Hexagonal, Cubic, and Lamellar Silica–Surfactant Mesophases That Are Precursors to M41S Materials**

type	silicon/ surfactant ratio	$T(^{\circ}\text{C})$	observations and comments
original MCM-41	3.6	150	< 1 h. Solid-phase rapid separation of solid phase from the solution phase. Growth of hexagonal phase with $d_{100} = 39.6 \text{ \AA}$ , 1 h after hydrolysis of TEOS. Phase identical to that of Si/Surfactant ratio 0.6 appears after 20 min of hydrolysis at room temperature. Heating to $100^{\circ}\text{C}$ results in the transformation to the lamellar phase. Hexagonal phases observed after induction times of 20 and 30 min, respectively.
TEOS MCM-41 (hex)	0.6	100	
TEOS MCM-50 (lamellar)	1.3	100	
dilute MCM-type reaction	4.3	65 and 75	

**Figure 10.** Stacked plot of the in situ EDXRD spectra of  $\text{Si}(\text{OEt})_4\text{--C}_{16}\text{TMACI/OH}$  reactions: (a) silicon/surfactant ratios = 0.6 showing the formation of the hexagonal phase and (b) silicon/surfactant ratios = 1.3 formation of the lamellar phase.

patterns of the phases obtained from these reactions is shown in Figure 11. Figure 10b appears to show a phase transformation after longer time periods. If the 40 Å phase for this reaction is hexagonal, as the appearance suggests, then a hexagonal to lamellar phase conversion occurs for this TEOS–surfactant mixture. The as-synthesized product recovered by filtration was lamellar, with  $d_{001} = 35.2 \text{ \AA}$  (Figure 11). Steel et al.<sup>8</sup> reported the detection of a hexagonal mesophase by  $^{14}\text{N}$  NMR spectroscopy in a silicate–surfactant gel with a Si/Sur

**Figure 11.** X-ray powder diffraction patterns of the products obtained from the  $\text{Si}(\text{OEt})_4\text{--C}_{16}\text{TMACI/OH}$  reactions: calcined hexagonal M41S, calcined lamellar M41S, and lamellar M41S.

ratio appropriate for the formation of a lamellar phase. After the gel was heated to  $90^{\circ}\text{C}$  in situ and cooled, the hexagonal phase disappeared and a product displaying lamellar topology was obtained. In this case, the cooperative organic–inorganic assembly may favor the formation of a hexagonal phase at lower temperatures. For these, higher silicate–surfactant ratios the silicate layers forming as a consequence of cooperative assembly may be too thick to cross-link effectively, until an increase in temperature which encourages the formation of a surfactant bilayer and hence the lamellar product. Removal of the surfactant by calcination caused structural collapse. The results of the study of M41S-type reactions by the in situ X-ray diffraction technique are summarized in Table 4.

## Conclusions

In situ energy-dispersive X-ray diffraction proved to be an extremely useful technique in the investigation of mesoporous material formation. Despite the large  $d$  spacings/low  $2\theta$  values involved and the inherent disordered nature of the materials, the short acquisition times and quality of the data collected on Station 16.4 permitted a detailed analysis of the silica–surfactant mesophases that are the precursors to mesoporous silicates. Qualitative interpretations of the in situ X-ray diffraction data suggest that the silica–surfactant mesophases formed are highly dependent on the reactant medium, the effect of the silica source being one of the main determining factors. Kanemite, a layered polysilicate, has proven to be an excellent silicate source, giving

rise to a relatively ordered mesophases and subsequent highly ordered mesoporous silicate products. The results obtained from the time-resolved X-ray diffraction data of the kanemite–alkyltrimethylammonium system are consistent with previous mechanistic studies of this material. The silica–surfactant mesophase precursor to FSM-16 forms from a medium containing a number of intercalated silicate phases, while in contrast, the hexagonal mesophase precursor to MCM-41 forms from a medium containing no other ordered silicate–surfactant phases detectable by in situ X-ray diffraction.

**Acknowledgment.** The authors acknowledge financial support from the EPSRC, Leverhulme Trust, British Council and Grant-in-Aid by the Ministry of Education, Science and Culture of the Japanese Government. We thank the staff at Daresbury for their considerable assistance: Dr. S. M. Clark, A. Nield, and M. Miller. S.O'B thanks Dr. M. J. Rosseinsky for advice and Dr. M. Morey for useful discussions. We also acknowledge the late A. Monnier in recognition of his important contribution to this field of research.  
CM990044A